Spectrochimica Acta, Vol. 45A, No. 4, pp. 409–419, 1989.
Printed in Great Britain.

0584 8539/89 \$3.00+0.00

Infrared spectra of $B(OMe)_3$, $ClB(OMe)_2$ and Cl_2BOMe species, isolated CH stretching frequencies and bond strengths

D. C. McKean and A. M. Coats
Department of Chemistry, University of Aberdeen, Aberdeen AB9 2UE, U.K.

(*Received* 15 *August* 1988; *accepted* 2 *November* 1988)

Abstract—Infrared spectra in the gas phase are reported over the range 3100–500 cm^{-1} for species of $B(OMe)_3$, $ClB(OMe)_2$ and Cl_2BOMe, with CH_3, CD_3 and CHD_2 substitution. A detailed analysis of νCH and νCD data in all three species of Cl_2BOMe yields strong evidence for the presence of three kinds of CH bond, two of them weak and one of them strong. The methyl group is then twisted, probably through 10–20°, out of the eclipsed or staggered conformation. The CHD_2 spectra of the di and trimethoxy compounds are less susceptible to analysis, but suggest also the presence of two weak and strong bonds, the former increasing in weakness as the number of methoxy groups increases. This is as expected from the increased competition likely between the lone pair electrons for the empty boron orbital. The spectra of the CD_3 species permit a clear assignment of νBO, δ_sCH_3, δ_sCD_3 and $\delta_{as}CD_3$ modes. In $Cl(COCH_3)_2$, ν_sBO lies at 1278 cm^{-1}.

INTRODUCTION

Studies of "isolated" CH stretching frequencies, ν^{is}_{CH}, measured in partially deuterated compounds, have shown that in CH_3–O–X compounds there are generally two and occasionally three types of CH bond [1–3]. Of these, the two which lie *trans* to the oxygen lone pairs are weak, while the one which lies *trans* to the O–X bond is strong. The strong–weak difference varies considerably, from 101 cm^{-1} in Me_2O [1] to 23 cm^{-1} in $MeONO_2$ [4], the presence or lack of conjugation of the oxygen lone pair appearing to exert an important influence. In compounds involving the MeO–B group, the loss of oxygen electrons to the vacant boron orbital may similarly be expected to reduce the bond strength asymmetry.

Amongst the $Cl_nB(OMe)_{3-n}$ compounds selected here for study ($n=0, 1, 2$) the only one for which an experimental structure is available is $B(OMe)_3$. Electron diffraction shows this compound to have a planar skeleton with each methyl group twisted through either 23.0° [5] or 31.0° [6] from an eclipsed configuration.

It may be surmised however that the $ClB(OMe)_2$ and Cl_2BOMe structures resemble those of $MeB(OMe)_2$ and Me_2BOMe respectively. These both have planar skeletons, the former existing in a *syn/anti* conformation [6]. There appears to be slight evidence that the methyl groups in each case are staggered [6]. That the planarity arises also from B–Cl double bond character, to a small extent, is suggested by ^{35}Cl NMR spectra [7].

Other structural studies of these compounds include electric dipole moments [8] and ^{11}B and ^{1}H NMR spectra ([9] and references in [8]).

Previous spectroscopic work is limited to naturally occurring species only. Infrared and Raman data for $B(OCH_3)_3$ are analysed by Rogstad *et al.* [10]. $ClB(OCH_3)_2$ and Cl_2BOCH_3 have been studied in the i.r. by Lehmann *et al.* [11] and in both i.r. and Raman by De Moor *et al.* [12], differences of opinion appearing on the location of the νBO modes in the dimethoxy compound.

The present work has two objectives: to throw light on the structure of the methyl group through ν^{is}_{CH} studies, and to clarify some of the assignments below 1600 cm^{-1}. Achieving the latter objective is indeed important in reaching the former, since a necessary part of the analysis of CHD_2 spectra is their relation to those of CH_3 and CD_3, for which purpose an understanding of the Fermi resonances with $2\delta_s$Me and $2\delta_{as}$Me is needed. This is harder than usual in these MeOB compounds in view of the presence of νBO modes in the region where $\delta_{as}CH_3$ and δ_sCH_3 modes are usually found.

EXPERIMENTAL

While standard methods are available for preparing $B(OMe)_3$, $ClB(OMe)_2$ and Cl_2BOMe [13], the preparation of these compounds on a millimolar scale presented difficulties not mentioned by earlier workers. Thus the starting material, BCl_3, could not be completely separated from Cl_2BOMe by fractional condensation, and our samples of the latter contained small amounts of the former which obscured the 1000–950 cm^{-1} region. Similarly, bands due to traces of methanol were observed in the $B(OMe)_3$ spectra. The trimethoxy samples were made in quantitative yield by condensing a slight excess of methanol with BCl_3 at 75 K, warming to −85°C for about 30 min before fractionating through baths at −90° and −196°. The chloromethoxy compounds were made in a similar way by reacting $B(OMe)_3$ and BCl_3 in the appropriate proportions. Certain of the Cl_2BOMe samples contained, in addition to BCl_3, some $ClB(OMe)_2$, identified by the strong bands at 1276 and 1031 cm^{-1}, clearly absent in the spectra of the sample shown in Fig. 1. Similar bands at 1280 and 1030 cm^{-1} appear strongly in the i.r. spectrum of Cl_2BOMe in Fig. 1 of [12] and to a lesser extent in the spectrum in [11]. However the impurity undoubtedly present in the former spectrum does not appear to have been $ClB(OMe)_2$ judging by the absence

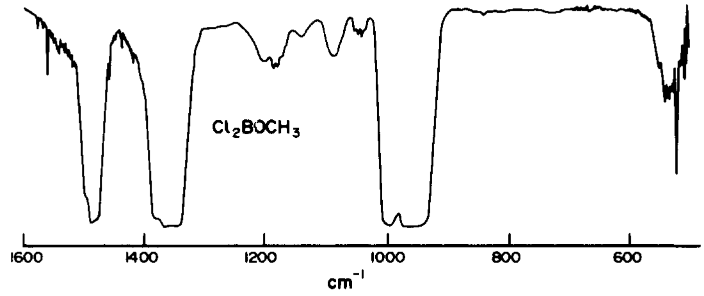

Fig. 1. Infrared spectrum of Cl_2BOCH_3, 1600–475 cm^{-1}.

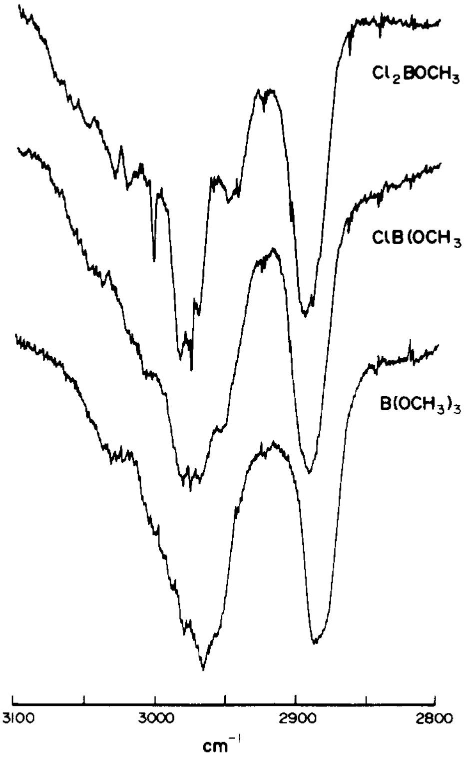

Fig. 2. νCH region for $B(OCH_3)_3$, $ClB(OCH_3)_2$ and Cl_2BOCH_3.

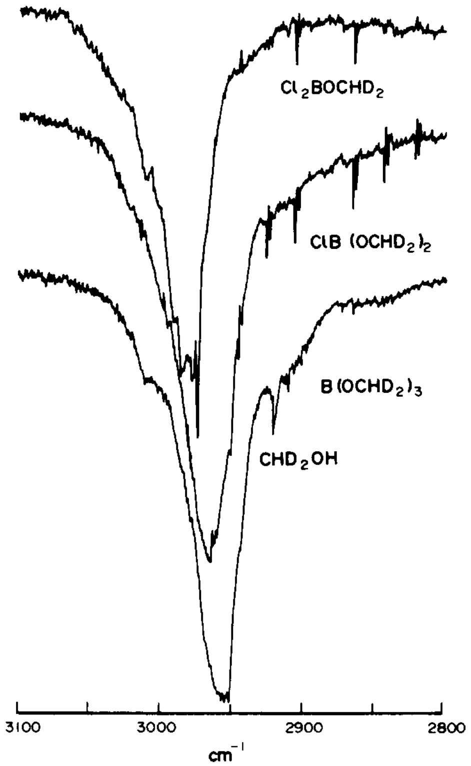

Fig. 3. νCH region for $B(OCHD_2)_3$, $ClB(OCHD_2)_2$ and Cl_2BOCHD_2. HCl and CHD_2OH absorptions are also present.

of the characteristic $ClB(OMe)_2$ bands near 600 cm^{-1}. In other respects our spectra were similar to earlier ones.

Bands due to HCl and DCl were always present in the spectra of our chloromethoxy samples and were removed by subtraction with variable success.

All spectra were recorded in the vapour phase on a Nicolet 7199 FTIR spectrometer, normally operating at a resolution of 0.5 cm^{-1}, but in a few cases at 1.0 cm^{-1}.

RESULTS AND DISCUSSION

The i.r. spectra obtained are illustrated in Figs 1–6, and the frequencies found in Tables 1–9. A detailed analysis proved to be possible for the monomethoxy compound, and this is considered first.

Cl_2BOMe; νCH/νCD

The spectra here show a number of well-defined band contours and a prediction of their appearance is therefore needed as a preliminary. Using an assumed geometry as shown in Fig. 7, moments of inertia were calculated for both staggered and eclipsed conformations of the methyl group. The *A* axis lies within 4°–9° of the CO bond, depending on the conformation and on the isotopic species chosen. Table 10 shows the angles made with respect to the *A*, *B* and *C* axes by each of the CH bonds in the methyl group, for the

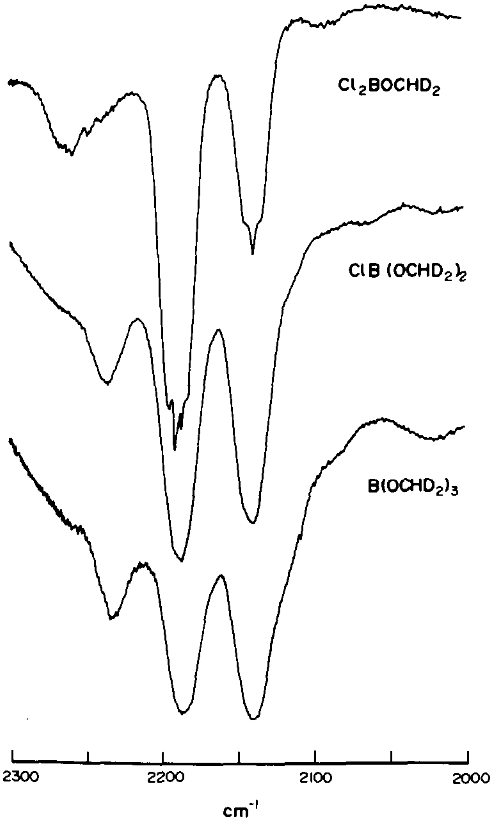

Fig. 4. νCD region for $B(OCHD_2)_3$, $ClB(OCHD_2)_2$ and Cl_2BOCHD_2.

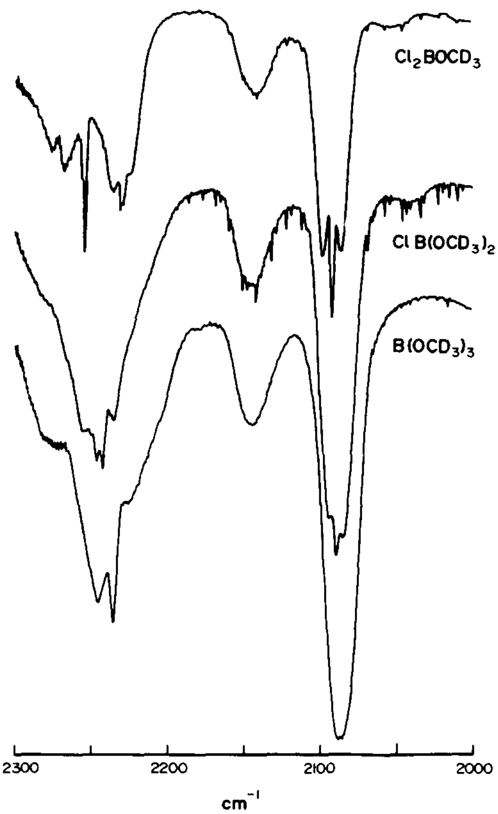

Fig. 5. νCD region for $B(OCD_3)_3$, $ClB(OCD_3)_2$ and Cl_2BOCD_3. DCl lines are also present.

eclipsed ($\phi H_1COB = 0°$) and staggered conformations ($\phi H_1COB = 180°$), and also for one rotated through 30°. From the calculated moments of inertia, using the diagrams of UEDA and SHIMANOUCHI [15], wing separations of about 12.6 and 8.0 cm^{-1} were estimated for type *A* and type *B* bands respectively. For the staggered and eclipsed forms, A'' vibrations should give rise to pure type *C* bands, whereas A' ones give *A*/*B* hybrids. Of the latter, a mode like $\delta_s CH_3$ should give an almost pure type *A* band, whereas $\nu_{as}CH_3$ or CD_3 (A') produces a dipole change rather close to the *B* axis.

Looking now at the spectra of the Cl_2BOCHD_2, Fig. 3, what appear to be three distinct bands are seen near 3000 cm^{-1}, a *B*/*C* one with wing spacing of about 8 cm^{-1} and weak *Q* branch at 3006.3 cm^{-1}, an *A*/*B*/*C* one at 2985.1 cm^{-1} and a type *C* with strong narrow *Q* branch at 2974.1 cm^{-1}. Since in either the eclipsed or staggered conformations only two types of CH bond could be present, a strong CH_s one and two CH_a ones, out of the plane, the presence of three bonds indicates a twist with ϕ (H_1COB) slightly different from either 0° or 180°, such that the two weak CH bonds are of slightly different strength. In so far as the eclipsed configuration puts the CH_1 bond closer to the *B* axis (10°) then the staggered one (26°) and the wing separation of the 3006.3 cm^{-1} bond is apparently *B*-type,

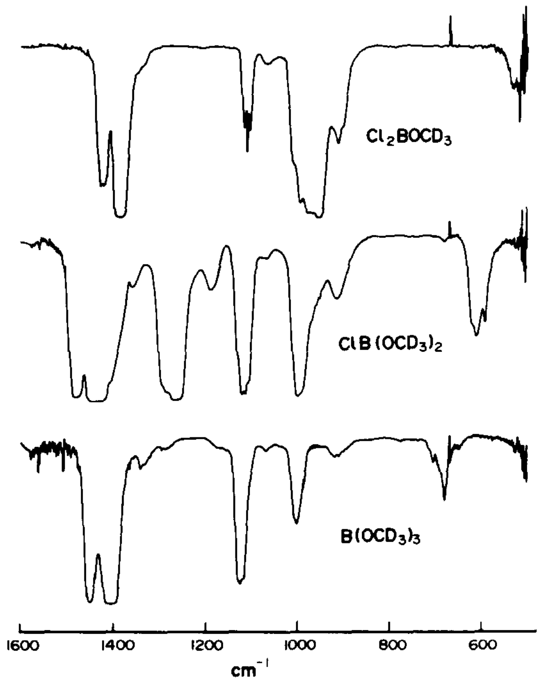

Fig. 6. Infrared spectra, 1600–475 cm^{-1}, of $B(OCD_3)_3$, $ClB(OCD_3)_2$ and Cl_2BOCD_3. Bands due to BCl_3 occur at 995 and 955 cm^{-1} in the Cl_2BOCD_3 spectrum.

Table 1. Gas phase i.r. frequencies (cm^{-1}) in Cl_2BOCH_3*

$\nu_{obs.}$	Assignment	$\nu_{obs.}$	Assignment
3050 sh		1202 sh	
3030.3		1186.6	
3026.5 min m, *B*	$\nu_{as}CH_3$ (*a*′)	1180.9 q m	ρCH_3
3021.8		1179.1 q	
3003.0 *Q*, m, *C*	$\nu_{as}CH_3$ (*a*″)	1173.6 sh	
2983.7		1164.4 sp, sh	
2975.7 q ms, *A*		1139 w	
2971.0	ν_sCH_3,	1086 m	νCO
	$2\delta_sCH_3$,		
2943.4 q, m, *A*	$2\delta_{as}CH_3$(*a*′),	1047.0 q w	2 × 521
2927 vw	$2\delta_{as}CH_3$ (*a*″)	1041.8 q	
2889.6 q, ms, *A*		996 vs	(^{10}B)
2739 vw, bd	2 × 1382	965 vvs	$\nu_{as}BCl_2$(^{11}B)
2691 w, bd	2 × 1354	838.5 q, vw	
2465 vw, bd		810 bd, vw	2 × 410
2030 vw, bd	535 + 1496?	727.5 q vw	475 + 262
~1975 w	521 + 1480?	721.3 q	200 + 521
1920 sh	(^{10}B)	550 q	$\delta_{\perp}OBCl_2$(^{10}B)
1892 w	1480 + 410 (^{11}B)	535 ms	ν_sOBCl_2
	1354 + 535		
~1496 sh	δ_sCH_3(^{10}B)	521.1 s *Q*, *C*	$\delta_{\perp}OBCl_2$(^{11}B)
1480.3 q, vs, *A*	δ_sCH_3(^{11}B)		
1381 sh	$\nu^{10}BO$		
~1354 bd, vvs	$\nu^{11}BO$		

*Resolution 0.5 cm^{-1}. (*a*′) and (*a*″) refer to the local methyl group symmetry.

Table 2. Infrared frequencies (cm^{-1}) in Cl_2BOCD_3

$\nu_{obs.}$(gas)	Assignment	$\nu_{obs.}$(gas)	Assignment
2826 vw	2 × 1421	1585 vw	
2756 w	2 × 1385	1510 vw	
2276 mw		1424 s, q	$\nu^{10}BO$
2272.2 min *B*	$\nu_{as}CD_3$(*a*′)	1385 vs, q	$\nu^{11}BO$
2268 mw		1340 sh	
2254.7 m, *Q*, *C*	$\nu_{as}CD_3$(*a*″)	1210 vw	
2231.3 m, q, *A*	2 × 1111.4	1111.4 s, *Q*, *A*	δ_sCD_3
2142 w	2 × 1066	~1066 w	$\delta_{as}CD_3$
2092.4 ms, *Q*, *A*	ν_sCD_3	1010 sh	
2155 vw		996 sh	BCl_3
2110 vw		980 sh	νCO?
1950 vw	536 + 1424	956 vs	BCl_3
1911 w	536 + 1385	909 s	ρCD_3
1892 sh	518 + 1385	807 vw, bd	
1647 vw		622 vw	
		~536	ν_sOBCl_2
		518.3 s, *Q*, *C*	$\delta_{\perp}OBCl_2$

there is perhaps slight evidence in favour of an eclipsed structure. However twisting the methyl group rapidly removes the distinction, and the wing spacing is in any event very approximate, since the band is situated on a sloping background of absorption. The only alternative explanation for the peaks between 2991 and 2974 cm^{-1} is a sequence of hot bands, starting from 2974.1 cm^{-1}, but the pattern of intensity distribution and the varying widths of the maxima make this rather unlikely.

The presence of three different CH bond strengths means that in principle three different $\nu_{as}CD_2$ and ν_sCD_2 frequencies would be expected for the CHD_2 group. It is in fact possible to detect three features associated with the $\nu_{as}CD_2$ band at ~2258 cm^{-1} (Table 3), although they are barely visible in the spectra of Fig. 4, and their positions agree quite well with those predicted by the refinement below. By contrast, in the ν_sCD_2 band at 2191 cm^{-1}, only a second additional feature is seen, at 2186.8 cm^{-1}. However this band is in strong resonance with $2\delta_sCD_2$ at 2139.6 cm^{-1} and the effects of this on the possible splittings of ν_sCD_2 are unpredictable.

Strong support for the presence of one strong and

Table 3. Infrared frequencies (cm^{-1}) in Cl_2BOCHD_2

3010 *R*	w, *A*	$\nu CH(HDD)$	1435 sh	$\nu^{10}BO$
3006.3 q			1404 vvs	$\nu^{11}BO$
~3000 *P*			~1355 sh	δCH?
2990.5 sh		$\nu CH(DHD)$	1326 q, vs, *A*	δCH
2985.1 m			1185 xw	
2977.6 m			1111.3 q, vw	
2974.1 m, *Q*, *C*		$\nu CH(DDH)$	1081.3 q, m	$\delta_s CD_2$
			~1015 sh	
2710 vw		1404 + 1326	996 sh	(BCl_3)
2261.8 q?		$\nu_{as}CD_2(DDH)$	~980 sh	νCO
2258.1 q, w		$\nu_{as}CD_2(DHD)$	~955 vs	(BCl_3)
2247.4 q, w		$\nu_{as}CD_2(HDD)$	920 sh	ωCD_2
2191.0 q, m		$\nu_s CD_2$	800 xw	ρCD_2
2186.8 q, m			625 xw	
2139.6 q, mw		2 × 1081	595 xw	
2100 xw			531 m	$\nu_s OBCl_2$
1936 w		531 + 1404	519.2 *Q*, m	$\delta_\perp OBCl_2$
1874 w				
1615 vw				

Table 4. Infrared frequencies in $B(OCH_3)_3$ near $3000\ cm^{-1}$*

$\nu_{obs.}$	Assignment
3030 sh	$\nu_{as}CH_3$ (*a*′)
2980 q	$\nu_{as}CH_3$ (*a*″)
2966 s, bd 2885 s	$\nu_{as}CH_3$, $2\delta_s CH_3$, $2\delta_{as}CH_3$
2815 w, bd, sh	

*Other frequencies were similar to those reported in [10]. (*a*′) and (*a*″) refer to the local methyl group symmetry.

two weak CH bonds comes from the spectra of the CH_3 and CD_3 species. These both show (Figs 2 and 5) a high frequency type *B* band (CH_3 3026.5, CD_3 2272.2 cm^{-1}) and a lower frequency type *C* one (CH_3 3003.0, CD_3 2254.7 cm^{-1}) followed by a complex of bands of predominantly *A* character which clearly derive from ν_sMe in resonance with $2\delta_s$Me and $2\delta_{as}$Me levels. The type *B* and *C* bands are readily assigned to $\nu_{as}(a')$ and $\nu_{as}(a'')$ respectively. The order $\nu_{as}(a') > \nu_{as}(a'')$ invariably reflects the presence of two weak and one strong bond, as all our previous partial deuteration studies have shown. This compatibility with the CHD_2 spectra is best revealed in a "3 × 3" refinement of all the CH and CD stretching frequencies (see further below). First however, we must assess the Fermi resonances, for which purpose we need to consider assignments below $1600\ cm^{-1}$.

Table 5. Infrared frequencies (cm^{-1}) observed in $B(OCD_3)_3$*

$\nu_{obs.}$	Assignment	$\nu_{obs.}$	Assignment
2899 vw, bd	2 × 1449	1449 vs	$\nu_{as}{}^{10}BO_3 e'$
2805 w, bd	2 × 1404	1404 vvs	$\nu_{as}{}^{11}BO_3 e'$
2736 vw, bd		1349 sh	
2574 vw		1283 w	
2493 vw		1170 sh	
2405 vw		1120 s	$\delta_s CD_3$
2360 q		1066 w	$\delta_{as}CD_3$
2280 sh	$\nu_{as}CD_3(a')$	1000.6 ms	$\nu COe'$
2245.2 ms	2 × 1122	918.9 mw	$\rho CD_3 e'$
2235.5 q, ms	$\nu_{as}CD_3(a'')$	908.2 q, mw	$\rho CD_3\ a''$
2224 sh		~860 vvw	
2205 sh		775 w, q, *C*	
2144 m	2 × 1066	701.9 m, q	$\delta_\perp{}^{10}BO_3 a''$
2086 ms	$\nu_s CD_3$	678.3 ms, q	$\delta_\perp{}^{11}BO_3 a''$
1994 w		648.3 mw, q	$\nu_{22} + \nu_{28}$
1945 sh			
1900 sh			
1805 vw			
1670 w			
1578 w			

*(*a*′), (*a*″) refer to the local methyl group symmetry, *e*′, *a*″ to the overall symmetry, assumed to be C_{3h}.

Table 6. Infrared frequencies (cm^{-1}) observed in $B(OCHD_2)_3$

$\nu_{obs.}$	Assignment	$\nu_{obs.}$	Assignment
3012 w, sh	νCH_i^*	1386 s	δCH
2967?, sh		1326 vs	δCH
2956.0 max, ms	$\nu CH_o\dagger$	1186 m	
2954.3 q, ms		1179 q, m	
2950.4 q, ms		1171 q, m	
2265 bd, sh	$\nu_{as}CD_2$	1143 m	νCO?
2233 w, bd	$\nu_{as}CD_2(HDD)$	1091 ms	$\delta_s CD_2$
2186 mw, bd	$\nu_s CD_2, 2\delta_s CD_2$	1044 ms	νCO
2140 mw, bd		993 mw, *A*	
2018 vw		925 w	
1675 vw		846 w	
1460 vs	$\nu_{as}{}^{10}BO_3$	703 q, sh	$\delta_\perp{}^{10}BO_3$
1422 vvs	$\nu_{as}{}^{11}BO_3$	681. q, m	$\delta_\perp{}^{11}BO_3$
		657 m	
		650 q, m	$\nu_{22}+\nu_{28}$

*Bond lying in, or close to, the skeletal plane.

†Bonds lying distant from the skeletal plane.

Table 7. Infrared frequencies (cm^{-1}) observed in $ClB(OCH_3)_2$

$\nu_{obs.}$	Assignment	$\nu_{obs.}$	Assignment
3038.5 sh	2 × 1522?	1522 sh	$\delta_s CH_3/\nu_{as}^{10}BO_2$
3006 sh	2 × 1502?	1502 vs	$\delta_s CH_3/\nu_{as}^{10}BO_2$
2981		~1465 sh	$\delta_{as}CH_3$
2975.6 q ms	$\nu_s CH_3$	1375 vvs	$\nu_{as}BO_2/\delta_s CH_3$
2968.5		1300 sh	
2954 sh		1278 vs	$\nu_s BO_2$
2891 bd, ms	2 × 1065	1167 ms	ρCH_3
2645 vw	1375 + 1278	1027 vs	νCO
2535 vw	2 × 1278	1002 sh	
2290 vw		646.1 q, m	νBCl
2140 vw		636.5 m	
2092 vw		616.3 q, w	$\delta_\perp{}^{10}BO_2Cl$
~2010 vw		594.8 m, *C*	$\delta_\perp{}^{11}BO_2Cl$
1911 vw			
~1770 vw			
~1650 vw			

Table 8. Infrared frequencies (cm^{-1}) observed in $Cl(BOCD_3)_2$

$\nu_{obs.}$	Assignment		
2850 vvw, bd	2 × 1434	1477 s	$\nu_{as}{}^{10}BO_2$
2760 vvw, bd		1434 vvs	$\nu_{as}{}^{11}BO_2$
2684 vw, bd		1405 sp, sh	
~2285 sh, bd	$\nu_{as}CD_3(a')$	1360 sh	
~2270 infl		1286 sh	$\nu_s{}^{10}BO_2$
2255 sh		1264 vs	$\nu_s{}^{11}BO_2$
2246.9 q	$\nu_{as}CD_3(a'')$	1188 m	
2242.9 q ms		1118.6 q	$\delta_s CD_3$
2236.2 q	$2\delta_s CD_3$,	1113.7 q s	
2145 m, bd	$2\delta_{as}CD_3$,	1108, 9 sh	
2088.9 ms, *A*	$\nu_s CD_3$	1066.5 w	$\delta_{as}CH_3$
2043 vw		997 s	νCO
1918 vw		959.5 sh	ρCD_3?
1874 vw		953 sh	
1723 vw		915.4 m	ρCD_3
1570 vw		680 vw	
		617 sh	νBCl
		609.1 ms	
		592.2 ms, q, *C*	$\delta_\perp BO_2Cl$

Table 9. Infrared frequencies (cm^{-1}) observed in $ClB(OCHD_2)_2$

$\nu_{obs.}$	Assignment	$\nu_{obs.}$	Assignment
3022 sh	$\nu CH(HDD)$?	1488 vs	$\nu_{as}{}^{10}BO_2/\delta CH$
2995 sh	νCH (DHD)	~1445 vvs	$\nu_{as}{}^{11}BO_2/\delta CH$
2977 sh	$\nu CH(DDH)$	1360 sh	δCH?
2964 ms		1328 vs	$\delta CH/\nu_{as}BO_2$
		1253 vs	$\nu_s BO_2$
2695 vw		1187 m	
~2265 sh, bd	$\nu_{as}CD_2$ (DDH)	1180 sh	
2235 m	$\nu_{as}CD_2$ (HDD)	1163 sh	
2187 ms	$\nu_s CD_2, 2\delta_s CD_2$	1091 s	$\delta_s CD_2$
2141 ms		1036 s	νCO
2070 vw		969 ms	νCO?
1970 vw, bd		919 sh	
1878 vw		690 vw	
1710 vw		660 sh	
		624 ms	νBCl
		593.1 ms, q, *C*	$\delta_{\perp}{}^{11}BO_2Cl$.

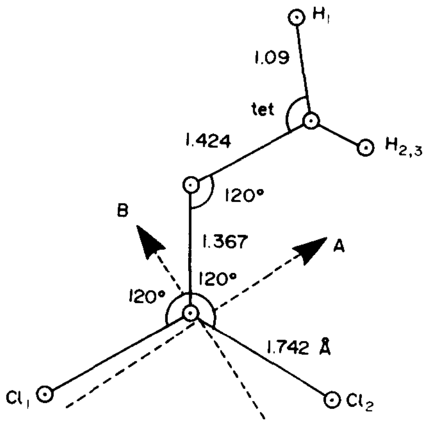

Fig. 7. Assumed geometry and directions of inertial axes in the staggered form of Cl_2BOCH_3 ($\phi H_1COB = 180°$). Bond lengths from BCl_3 [14] and $B(OMe)_3$ [5].

Cl_2BOMe: assignments below 1600 cm^{-1}, and Fermi resonances higher up

The B–O stretching frequency is only seen effectively isolated in the CD_3 species, where it produces the ${}^{11}B$ and ${}^{10}B$ bands at 1385 and 1424 cm^{-1} respectively (Fig. 6). In the CH_3 species this motion will couple strongly with $\delta_s CH_3$, but not with $\delta_{as}CH_3$. The 39 cm^{-1} boron isotope shift is then divided between the νBO bands at 1354 and 1381 cm^{-1} and the coupled $\delta_s CH_3$ ones at 1480.3 and ~1496 cm^{-1}. Back in the CD_3 species, $\delta_s CD_3$ will couple strongly with νCO and be found substantially higher than $\delta_{as}CD_3$, as in $(CD_3)_2O$ [16]. It is easy then to identify it with the pure type *A* band at 1111.4 cm^{-1}. $\delta_{as}CD_3$ is expected at about 1000 cm^{-1}, and is clearly responsible for the weak band at 1066 cm^{-1}. $\delta_{as}CH_3$ is then predicted to be at about 1465 cm^{-1} where it will be submerged by the much stronger $\delta_s CH_3$ band. We then estimate $\nu_s^0 CH_3$ and $\nu_s^0 CD_3$ as follows:

$$\begin{aligned}\nu_s^0 CH_3 &= 2975.7 + 2943.4 + 2889.6 \\ &\quad -(2\times 1465 - 10) - (2\times 1480.3 - 10) \\ &= 2938\ cm^{-1}\end{aligned}$$

$$\begin{aligned}\nu_s^0 CD_3 &= 2231.3 + 2142 + 2092.4 \\ &\quad -(2\times 1111.4 - 7) - (2\times 1066 - 7) \\ &= 2125\ cm^{-1}.\end{aligned}$$

In the CHD_2 species, the prominent band at 1081.3 cm^{-1} is clearly $\delta_s CD_2$, and we estimate $\nu_s^0 CD_2$ similarly:

$$\begin{aligned}\nu_s^0 CD_2 &= 2191.0 + 2139.6 - (2\times 1081.3 - 7) \\ &= 2175\ cm^{-1}.\end{aligned}$$

Discussing other assignments, a strong band at 1326 cm^{-1} in the CHD_2 species is clearly δCH coupled to a νBO mode displaced upwards to 1404 cm^{-1},

Table 10. Orientations of individual CH bonds with respect to inertial axes*

	A			*B*			*C*		
$\phi(H_1COB)$	0°	30°	180°	0°	30°	180°	0°	30°	180°
H_1	80	65	64	10	39	26	90	62	90
H_2	67	71	75	65	88	59	35	19	35
H_3	67	76	75	65	32	59	35	62	35

*Assuming *A* axis lies 6° from the CO bond.
$\phi = 0°$, 180° describe the eclipsed and staggered forms respectively.
For $\phi = 30°$, atom H_2 lies in a plane at right angles to the skeletal one.

Table 11. "3 × 3" refinement of νCH and νCD in Cl_2BOMe species

	$\nu_{obs.}$	σ_ν	ε		$\nu_{obs.}$	σ_ν	ε
CH_3	3026.5	1	0.0	CHDD	3006.3	1	0.0
	3003.0	1	−0.1		2247.4	10	−3.8
	2938	50	10.4		2170.8	50	7.2
CD_3	2272.2	5	1.8	CDHD	2985.1	1	0.0
	2254.7	5	3.8		2258.1	20	−6.3
	2125	50	0.3		2175.0	50	8.8
	f_1	4.9435		CDDH	2974.1	1	0.0
	f_2	4.8743			2261.8	10	−6.0
	f_3	4.8384			2175.0	50	4.1
	f'_{12}	0.0303					
	$f'_{13}=f'_{23}=f'_{12}$ constrained						

Geometry assumed: $H_1CH_2 = H_1CH_3 = 109.24°$; $H_2CH_3 = 107.72°$.

from its value of 1385 cm^{-1} in the CD_3 species. A weak shoulder near 1355 cm^{-1} may arise from another δCH vibration.

The $\delta_\perp OBCl_2$ type C band near 520 cm^{-1} moves downward slightly in a progressive way with increasing number of deuterium atoms. The band just above, whose origin in $\nu_s BCl_2$ can scarcely be doubted from the Raman spectrum [12], has an indefinite contour and may also move on deuteration (the noise level here was very high). Whereas νCO clearly lies at 1086 cm^{-1} in the CH_3 species, it is probably obscured beneath the impurity BCl_3 bands in the CD_3 one. Bands near 1180 cm^{-1} (CH_3) and 909 cm^{-1} (CD_3) arise from ρMe vibrations. The possibility of significant splittings in these, as in Me_2O [16] should not be overlooked.

Cl_2BOMe: "3 × 3" refinement

The CH and CD stretches were refined on our usual energy factored force field approximation, where the effects of anharmonicity were ameliorated by dividing observed νCD values by 1.011 before input, and remultiplying the calculated ones after output to give the error vector $\varepsilon = \text{obs} - \text{calc}$ in Table 11. The initial calculation was for a C_s structure with two weak bond frequencies of 2974.1 cm^{-1} plus the strong one of 3006.3 cm^{-1} using an HCH angle borrowed from $B(OMe)_3$ [5]. This model has just two possible stretch–stretch interaction constants ($f'_{12} = f'_{13} \neq f'_{23}$) which both refined to about 0.022 mdyn/Å. This is lower than the normal value of about 0.03 mdyn/Å. The three different ν^{is}CH values chosen above were then introduced, with the same constraint on the interaction constants and the same HCH angle. This gave a satisfactory value of f'_{12} ($=f'_{13}$) of 0.0305 mdyn/Å but too high a value of f'_{23}, 0.040 mdyn/Å.

Recollecting that differences in interaction force constants can be removed by varying HCH angles in a manner which is supported by both microwave and *ab initio* studies of CH_3CXO compounds [17] we then allowed $\widehat{H_2CH_3}$ to vary until all the interaction force constants were identical. This is the refinement and force field shown in Table 11. The 1.52° difference needed in the HCH angle would appear to be somewhat larger than the smaller value of 0.6° in Me_2O found by an *ab initio* calculation [18] or the 0.8° in this molecule in the microwave r_s structure [19]. However we have reworked the latter data to give an r_0 structure, using the assumption $r_0(CH) - r_0(CD) = 0.002$ Å, and find $\widehat{H_aCH_s} = 110.0°$, $\widehat{H_aCH_a} = 108.2°$, a difference of 1.8°.

Be this as it may, the evidence for angular asymmetry in the methyl group of Cl_2BOMe is not as strong as it is in the CH_3CXO compounds.

A last feature of the refinement shown is the relatively good prediction of ν_s modes, which suggests that the analysis made above of the Fermi resonance is essentially correct.

ν^{is}_{CH} values and the twist angle ϕ

If the variation of ν^{is}_{CH} with twist angle were known, the observation of three ν^{is}_{CH} values would allow a determination of this angle. The simplest potential function applicable to a molecule such as CH_3NO_2 has only a V_2 term, and the frequencies of the individual bands are given by [20]

$$\nu CH_1 = \nu_0 + a\cos 2\phi$$

$$\nu CH_3 = \nu_0 + a\cos 2(\phi + 120°)$$

$$\nu CH_3 = \nu_0 + a\cos 2(\phi + 240°).$$

If this is applied to Cl_2BOMe, the three observed frequencies then give $\nu_0 = 2988.5$, $a = 18.9$ cm^{-1}, $\phi = 9.8°$ which seem not unreasonable.

However, in the only cases known to us where such potential functions have been determined, namely in CH_3Ph and CH_3NO_2, a substantial V_4 term is found to be present [21].

We therefore repeated the above calculation assuming equations such as $\nu CH_1 = \nu_0 + a\cos 2\phi + b\cos 4\phi$ and taking $b = 0.3a$.

The three observed frequencies are then fitted with a little altered at 20.2 cm^{-1}, but ϕ increased substantially to 18.5°. The reason for this is that addition of a positive $\cos 4\phi$ term increases the width of the minimum in the ν vs ϕ curve and diminishes that of the maximum. A larger ϕ is then needed to produce the observed splitting between the two weak CH bonds.

A further complication may arise since a V_1 term may also be present—in principle the νCH_1 frequencies of the eclipsed and staggered forms may differ. This further widens the range of ϕ compatible with the observed frequencies. All that can be said at this stage is that it would be relatively easy to reconcile the latter with a twist angle of 23.6° as reported initially for the methyl groups in $B(OMe)_3$ [5]. At this point however, the value of a required and the magnitude of b relative to a begin to increase very rapidly (see further, below).

Since an independent determination of the value of ϕ would lead back to the evaluation of two parameters in the functional variation of νCH, the result of a microwave study of the structure will be keenly awaited.

$B(OMe)_3$ and $ClB(OMe)_2$

The lack of well defined band centres and of Raman spectra together preclude here the type of detailed analysis achieved above for Cl_2BOMe. The CHD_2 spectra in the 3000 cm^{-1} region show a moderately strong, broad and asymmetric band, on the high frequency side of which several ill-defined shoulders may be seen (Fig. 3). The centre of this broad band moves to lower frequency as the number of methoxy groups increases. The general resemblance overall to the Cl_2BOCHD_2 spectrum leaves little doubt that also in the di and trimethoxy compounds, each methyl group has two weak and one strong CH bonds, with the weak ones becoming weaker in the sequence $OMe > (OMe)_2 > (OMe)_3$.

Other features of the spectra which support this interpretation are the splitting of $\nu_{as}CD_2$ into a broad shoulder at about 2265 cm^{-1} and a broad maximum at 2235 [$ClB(OCHD_2)_2$] or 2233 cm^{-1} [$B(OCHD_2)_3$], Fig. 4, and the sequence 2254.7–2246.9, 2242.9–2235.5 cm^{-1} followed by the type *C* bands arising from $\nu_{as}CD_3$ (a'') in the mono, di and trimethoxy compounds respectively (Fig. 5). Looking for the $\nu_{as}CH_3$ (a'') counterparts to these last CD_3 bands, a shoulder at 2980 cm^{-1} in $B(OCH_3)_3$ is in the right place, but that at 3006 cm^{-1} in $ClB(OCH_3)_2$ is not, and may have some alternative origin (see below). The expected downwards trend in the lowest CH_3 or CD_3 stretching frequency is not seen, which may be ascribed to the strong Fermi resonances present and to the fact that δ_sCD_3, δ_sCD_2, and by inference, δ_sCH_3, rise with increase in the number of methoxy groups, as shown for example in Fig. 6. This can be seen to increase the degree of Fermi resonance affecting ν_sCD_2 in the CHD_2 spectra of Fig. 4. It seems likely that here $\nu_s^0CD_2$ and $2\delta_sCD_2^0$ crossover between the mono and trimethoxy compounds.

By contrast with δ_sCD_3, $\delta_{as}CD_3$ stays remarkably constant at 1066 ± 1 cm^{-1}, and so presumably does $\delta_{as}CH_3$.

The earlier controversy over the assignment of the νBO modes [11, 12] in $ClB(OMe)_2$ is resolved by the observation of strong ^{11}B bands at 1434 (ν_{as}) and 1264 (ν_s) cm^{-1} in $ClB(OCD_3)_2$, confirming the assignment of LEHMANN *et al.* [11] and the similar assignments in $MeB(OCH_3)_2$ of GUNDERSEN *et al.* [6]. Figure 6 also shows that there is no simple trend in the νBO frequencies in the series, the highest of which is in the dimethoxy compound.* This may well be due to a G matrix effect rather than an F matrix one. If such is the case, an overlay force constant treatment of all three molecules might well reveal what is the skeletal conformation of the dimethoxy compound. By analogy with $MeB(OMe)_2$ this would be expected to be a *syn/anti* form with two non-equivalent methoxy groups. A hint of such a dissymmetry comes from the appearance of two *Q* branches attributable to $\nu_{as}CD_3$ (a'') at 2146.9 and 2242.9 cm^{-1} (Fig. 5).

Assignments elsewhere in the spectra are conventional. Bands near 1170 cm^{-1} are certainly due to ρCH_3, but the example of other molecules such as Me_2O [16] makes one hesitate to assume that all such modes lie there. Additional νCO modes remain to be identified, either through Raman spectra, or by using ^{13}C substitution.

The pattern of bands between 650 and 710 cm^{-1} in the $B(OMe)_3$ compounds suggests that $\nu_{22} + \nu_{28}$ is in Fermi resonance with $\delta_\perp BO_3$, lying below it in the CHD_2 and CD_3 species. In $B(OCH_3)_3$ however we suppose that it lies *above* $\delta_\perp{}^{11}BO_3$ but *below* $\delta_\perp{}^{10}BO_3$. This produces a more acceptable pattern of boron isotope shift than the interpretation of ROGSTAD *et al.* [10]. (We do not in fact observe the latter's peak at 670 cm^{-1}.) It also explains why $\delta_\perp{}^{11}BO_3$ *rises* from 667 cm^{-1} in $B(OCH_3)_3$ to 681 cm^{-1} or 678 cm^{-1} in the CHD_2 or CD_3 compounds.

Having described the broad features of the $ClB(OMe)_2$ and $B(OMe)_3$ spectra, we return to their CHD_2 νCH bands and enquire more closely as to the origin of the contours seen. A possible clue is found in the spectrum of $B(OCHD_2)_3$, where a succession of weak *Q* branches, 2950.4, 2954.3 and 2956.0 suggests a sequence of hot bands in very low lying vibrational states. The latter could be either methyl torsions, assigned at 230 and 195 cm^{-1} in $B(OCH_3)_2$, or the BOC twisting modes put at 165 and 102 cm^{-1} in the same molecule [10].

Either of these motions could, with increasing amplitude, lead to a blurring of the distinction between the two kinds of weak CH bond which would be present if the methyl group is slightly twisted away from the eclipsed or staggered configurations. Thus one kind, in the ground vibrational state would be represented by the *Q* branch at 2950.4, and the other by a shoulder at about 2967 cm^{-1}. The centre of the

---

*This produces an extra high δ_sCH_3 band at 1502 cm^{-1} (Table 6) whose overtone may be responsible for the shoulder at 3006 cm^{-1} in $ClB(OCH_3)_2$.

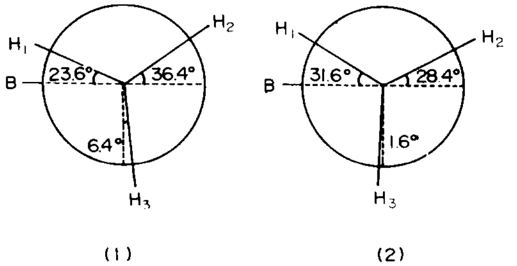

Fig. 8. Newman diagrams for the CH_3OB group: (1) ϕ (H_1COB) = 23.6°; (2) ϕ (H_1COB) = 31.6°.

Table 12. Isolated CH stretching frequencies (cm^{-1}) in OMe compounds

	H_1	H_2		H_3
Cl_2BOMe*	3006.3	2985.1		2974.1
$ClB(OMe)_2^*$	3022?		~2965	
$B(OMe)_3^*$	3012	2967?		2950.4
HOMe†	2979.2		2920.6	
CH_3OMe†	2984.8		2883.4	
Cl_2POMe‡	3017		2991	
HCOOMe§	3020.1		2981.0	
CH_3COOMe§	3012.3		2976.7	
O_2NOMe‖	3012.6		2989.3	
FCH_2OMe¶	3004	2957		2913
$ClCH_2OMe$¶	3005	2949		2913
$BrCH_2OMe$¶	3007	2945		2916
ICH_2OMe¶	3005	2930		2916

*This work.
†Ref. [22].
‡Ref. [1].
§Update of data in Ref. [1].
‖Ref. [4].
¶Ref. [23].
These are all from *gauche* skeletal conformers.

main band, ~2956 cm^{-1}, would then represent the average weak bond frequency over a substantial change of torsional angle. It seems possible that we have here a case of behaviour intermediate between what is observed in a high barrier situation, as in an ethyl halide or hydrocarbon, and a very low barrier one, as in toluene or nitromethane where the main band seen represents an average over an entire torsional cycle. At either extreme, the ν_{CH}^{is} contours seen are those of normal *A*, *B* or *C* type bands (or hybrids of these) as appropriate to the direction of the dipole derivative. In between, these characteristics are lost.

If this interpretation is valid, it casts some doubt on the more recent value of 31.6° for the dihedral HCOB angle ϕ which defines the twisting of the methyl group [6]. As shown in Fig. 8, this produces a conformation in which one CH bond is only 1.6° away from a plane perpendicular to the skeleton one, while the other two are at about 30° to the latter. For a simple V_2 potential in a normal CH_3 compound this would lead to two strong CH bonds and one weak in each case [2]. As we have seen in the case of Cl_2BOMe, the situation of two weak and one strong CH bond can be restored with $\phi \sim 20°$ if a sufficiently large V_4 term is added (30% of V_2). To achieve the same result for $\phi = 31.0°$ however would entail a much larger V_2 term (~80 cm^{-1}) and a V_4 one $\approx 0.85\ V_2$. These seem rather unlikely.

GENERAL DISCUSSION

Table 12 lists the isolated CH stretching frequencies determined in this work along with all earlier measured values for −OMe compounds. The results for the BOMe compounds most closely resemble those for methyl formate and acetate, where there is a similar loss of oxygen lone pair density through conjugation with the rest of the molecule. This we relate to a somewhat smaller strong–weak separation than is found, say, in Me_2O or $MeOCH_2X$. In keeping with this notion is the systematic fall in ν_{CH}^{is} for the out-of-plane bonds as the number of methoxy groups increases. The more competition there is for occupancy of the empty boron orbital, the less electron density will be donated by a particular oxygen, and the greater the weakening effect on the *trans* CH bonds. The evidence from the mono and trimethoxy compounds suggests that the strong CH bond is unaffected. Indeed the νCH_s value seems to be remarkably constant at around 3010 ± 10 cm^{-1}, except for methanol and dimethylether, where it falls to about 2980 cm^{-1}.

In conclusion, we note that predictions of r_0CH can be made from all these ν_{CH}^{is} values using the current correlation relation [2]

$$r_0CH = 1.3982 - 0.0001023\,\nu_{CH}^{is}$$

Acknowledgement—We thank the SERC for the FT-i.r. facility.

REFERENCES

[1] D. C. McKEAN, J. L. DUNCAN and L. BATT, *Spectrochim. Acta* **29A**, 1037 (1973).
[2] D. C. McKEAN, *Chem. Soc. Rev.* **7**, 399 (1978); *J. molec. Struct.* **113**, 251 (1984).
[3] D. C. McKEAN, I. TORTO and A. R. MORRISON, *J. molec. Struct.* **99**, 101 (1983).
[4] B. J. VAN DER VEKEN, M. A. HERMAN and D. C. McKEAN, *J. molec. Struct.* **114**, 27 (1984).
[5] G. GUNDERSEN, *J. molec. Struct.* **33**, 79 (1976).
[6] G. GUNDERSEN, T. JONVIK and R. SEIP, *Acta chem. scand. A* **35**, 325 (1981).
[7] K. BARLOS, J. KRONER, H. NÖTH and B. WRACKMEYER, *Chem. Ber.* **110**, 2774 (1977).
[8] J. E. DE MOOR and G. P. VAN DER KELEN, *J. organomet. Chem.* **9**, 23 (1967).
[9] J. E. DE MOOR and G. P. VAN DER KELEN, *J. organomet. Chem.* **6**, 235 (1966).
[10] A. ROGSTAD, B. N. CYVIN, S. J. CYVIN and J. BRUNVOLL, *J. molec. Struct.* **35**, 121 (1976).
[11] W. J. LEHMANN, T. P. ONAK and I. SHAPIRO, *J. chem. Phys.* **30**, 1219 (1959).
[12] J. E. DE MOOR, G. P. VAN DER KELEN and Z. EECKHAUT, *J. organomet. Chem.* **9**, 31 (1967).
[13] E. WIBERG and W. SÜTTERLIN, *Z. anorg. allg. Chem.* **202**, 1 (1931); *ibid.* **225**, 204 (1935).
[14] S. KONAKA, Y. MURATA, K. KUCHITSU and Y. MORINO, *Bull. chem. Soc. Japan* **39**, 1134 (1966).
[15] T. UEDA and T. SHIMANOUCHI, *J. molec. Spectrosc.* **28**, 350 (1968).

[16] A. Allan, D. C. McKean, J.-P. Perchard and M.-L. Josien, *Spectrochim. Acta* **27A**, 1409 (1971).

[17] D. C. McKean and I. Torto, *J. molec. Struct.* **81**, 51 (1982).

[18] J. E. Boggs, M. Altmann, F. R. Cordell and Y. Dai, *J. molec. Struct.* **94**, 373 (1983).

[19] H. Blukis, P. M. Kasai and R. J. Myers, *J. chem. Phys.* **38**, 2753 (1963).

[20] D. C. McKean and R. A. Watt, *J. molec. Spectrosc.* **61**, 184 (1976).

[21] D. Cavagnat and J. Lascombe, *J. molec. Spectrosc.* **92**, 141 (1982).

[22] J. L. Duncan, D. C. McKean, I. Torto, A. Brown and A. M. Ferguson, *J. chem. Soc. Faraday Trans. II* **84**, 1423 (1988).

[23] D. C. McKean, I. Torto and A. R. Morrison, *J. molec. Struct.* **99**, 101 (1983).